11th International Conference on Engineering Vibration
Ljubljana, Slovenia, 7–10 September 2015

A MECHANICAL MODEL FOR THE DYNAMICAL CONTACT OF ELASTIC ROUGH BODIES WITH VISCOELASTIC PROPERTIES

Frank Schulte*[1], Jan Neuhaus[2], Walter Sextro[2]

[1]Chair for Mechatronics and Dynamics, University of Paderborn, Germany
Frank.Schulte@uni-paderborn.de

[2]Chair for Mechatronics and Dynamics, University of Paderborn, Germany
{Jan.Neuhaus,Walter.Sextro}@uni-paderborn.de

Keywords: Contact Mechanics, Viscoelastic Material, Adhesive Friction, Hysteresis Friction, Energy Dissipation, Vibration.

Abstract. *The contact between viscoelastic materials e.g. elastomers and a rough surface leads to a special friction characteristic, which differs greatly in its properties comparing to other materials like metals. In practice, this friction combination occurs for example in the tire-road contact, or in the use of rubber gaskets. Due to the frictional forces a system is significantly influenced in its vibrational properties. The friction force is composed of two main components adhesion and hysteresis. The adhesion results from molecular bounds between the contact partners, while the deformation of the viscoelastic material by the roughness of the counter body leads to power loss. This internal friction results in an additional frictional force, which is described by the hysteresis.*

To simulate the frictional behaviour of elastomers on rough surfaces and thus to determine the energy dissipation in contact, it is necessary to develop a mechanical model which considers the roughness of the contact partners, as well as dynamic effects and the dependence on normal pressure and sliding speed. The viscoelastic material behaviour must also be considered. The contact between two rough surfaces is modelled as a rough rigid layer contacting a rough elastic layer. The elastic layer is modelled by point masses connected by Maxwell-elements. This allows the viscoelastic properties of the elastomer to be considered. The behaviour of whole system can be described by equations of motion with integrated constraints. The degrees of freedom of the model depends on the varying contact conditions. A point mass not in contact has two degrees of freedom. A point mass in contact moving along the roughness path can be described by only one degree of freedom. For each Maxwell-Element also an inner coordinate and thus a further degree of freedom is needed. Because of varying contact conditions during the simulation, the simulation interrupts in case the contact conditions change. Then the equations of motions are adapted with respect to the contact constraints.

As a result of the simulation one obtain the energy dissipation and thus the friction characteristic during the friction process. It is possible to use these results in three dimensional point-contact elements in order to model contact surfaces on lager length scales.

1 INTRODUCTION

Friction is the force resisting the relative motion of surfaces sliding against each other. The relative motion in the contact area leads to an energy transformation. The friction converts kinetic energy into thermal energy. Due to this energy dissipation friction plays an important role in dynamical engineering systems. There are different types of dynamic systems. In many systems the friction has to be minimized, so that wear is reduced and the lifetime is increased. On the other hand, there are dynamic systems, where the friction is used to reduce vibration amplitudes or to transmit forces. The reduction of vibration amplitudes leads in an increase of lifetime and safety due to a reduction of alternating stress. Another point is, that the noise development can be reduced, which depends on the vibration frequency and amplitude. For all this reasons, a good knowledge of friction phenomena is necessary to develop an optimized dynamic system.

Viscoelastic materials e.g. elastomers are used in many technical systems. An important field of application is, for example, tire road contact. Driving safety and comfort as well as occurring emissions depend on the contact conditions in the tire contact area. The complex material behavior of these materials results in an special friction characteristic. In the following publication, the elastomer friction is described. Then, the friction characteristics are explained with reference to viscous material properties. A corresponding contact model is presented based on these investigations.

2 ELASTOMER FRICTION

The friction characteristics of viscoelastic materials differ greatly in their properties comparing to other materials like metals. It is not possible to describe these contacts with classic friction laws. Parameter like sliding speed, surface pressure and temperature strongly influence the friction characteristic. Due to the low material stiffness, the elastomer penetrates into the free areas of roughness under normal pressure. This results in a large true contact area compared to other contact pairs, e.g. Steel-Steel. This again leads to high adhesive forces between the contact partners. Due to the material deformation during sliding energy is dissipated in the material which leads to so called hysteresis friction.

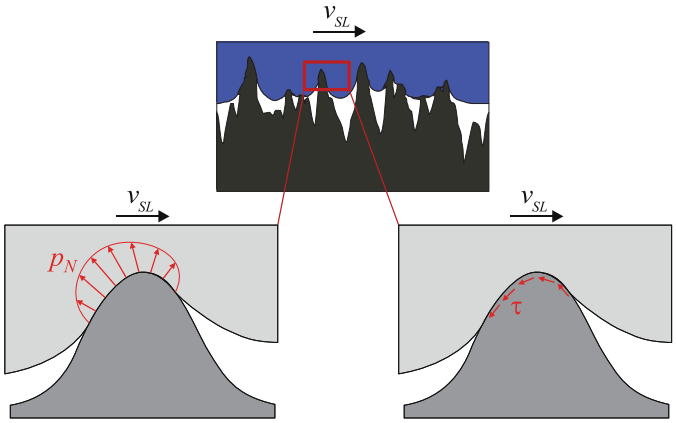

Figure 1: Hysteresis and adhesive friction of viscoelastic materials [1].

Figure 1 shows the two main effects of the friction viscoelastic materials adhesion and hysteresis, which are described in the following.

2.1 Hysteresis friction

The reason for hysteresis friction is the internal damping of viscoelastic materials. During sliding over the rough surface, the material is deformed. Due to the deformations, the material continuously braces and then relaxes again. This process is not adiabatic, so a part of the stored elastic energy is converted into heat. The dissipated energy results macroscopically in an increased frictional force.

The hysteresis friction is deformation-rate dependent. Depending on the roughness, which can be described as self-affine, there is an excitation by various frequencies in contact.These frequencies increase with rising sliding speed. Due to the rate-dependency of viscous properties the dissipated energy and thus the friction coefficient shows a maximum over sliding speed. This maximum is dependent on the wavelength of surface roughness.

2.2 Adhesive friction

Adhesive friction arises due to direct contact of the two friction partners. Between the viscoelastic material and the rough surface intermolecular bonds form, e.g. van der Waals bonds and hydrogen bonds [2]. Molecular compounds can be stretched before they are broken, thereby tension occurs. The constant breaking and formation of bonds is lossy and leads to a sliding resistance. Adhesive friction is directly dependent on the true contact area which again depends on the relative speed. At low speeds, the viscoelastic material can penetrate deeper into the roughness.

3 ELASTOMER PROPERTIES

Hysteresis and adhesive friction can be explained using the mechanical properties of viscoelastic materials. These are strongly dependent on the deformation rate and the temperature. If a sample is excited with a sinusoidal strain ε, results for the stress σ also a sinusoidal profile with a phase shift δ,

$$\begin{aligned} \varepsilon(t) &= \varepsilon_0 sin(\omega t), \\ \sigma(t) &= \sigma_0 sin(\omega t) + \delta. \end{aligned} \tag{1}$$

The relationship between stress and strain can be described by the complex modulus of elasticity E^*. Separation of real and imaginary part leads to

$$E^* = \frac{\sigma^*}{\varepsilon^*} = E^{'} + iE^{''}. \tag{2}$$

The real part $E^{'}$ is called storage module. This module describes the proportion, which oscillates with the excitation in phase. The imagninary part $E^{''}$ is called loss modulus and includes the part which vibrates $90°$ out of phase with the excitation. The storage and loss module are shown in Figure 2. For small excitation frequencies the storage module is lower compared to high frequencies. Thus the stiffness of the material increase with the frequency. The state above the frequency at which the dynamic stiffening takes place is called glass state. The loss modulus has a maximum in the range of the glass transition.

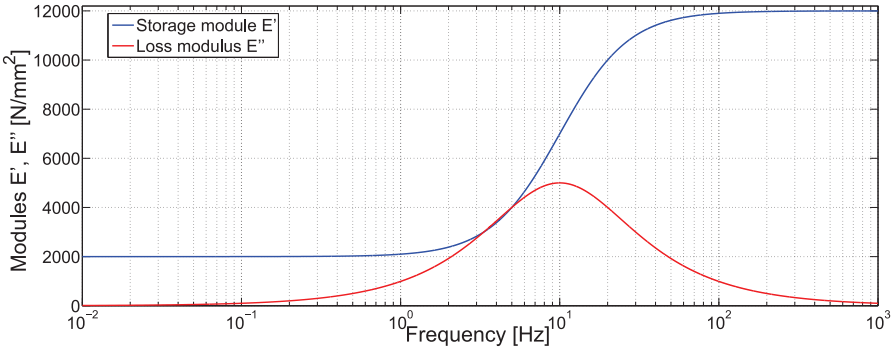

Figure 2: Schematic characteristic of storage and loss modulus.

Considering measured coefficients of friction as a function of relative velocity commonly two maxima are observed [3,4]. One maximum occurs at low speeds another one appears at higher velocities. This curve can be explained by the described effects. The first maximum can be explained by the adhesion. For low speeds the true contact area is large, so that many molecular bonds are formed. At higher velocities the material stiffens and the penetration depth decreases. Thus, the true contact area and the adhesive friction decrease. On the other hand the loss modulus increases, so the hysteresis component of friction increases. Where the loss modulus reaches its maximum, the second maximum of the friction value curve is formed.

To simulate the contact of an elastic body with viscoelastic properties a model is needed that reflects the deformation of the elastomer. For the hysteresis friction the dissipated energy must be calculated in the contact due to these deformations. To calculate the adhesive friction the true contact area needs to be determined. In the following a contact model is presented, which is able to simulate these properties.

4 CONTACT MODEL

The contact model is based on the approaches of [5,6]. The contact between a rough surface and a visoelastic material can be modelled in two dimensions as a rough rigid layer contacting a rough elastic layer. When considering the contact of an elastomer with a hard surface, the stiffness of the hard material can be assumed to be rigid. This is, for example, applicable to the contact tire-road or rubber-steel. As shown in Figure 3, the elastic layer is modelled by discrete elements, while the rigid surface is modelled continuously by cubic splines. The viscoelastic body is reduced to a thin layer modelled by k point-masses.

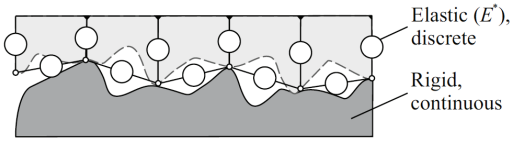

Figure 3: Modelling of two rough surfaces in contact [7].

Figure 4 shows the two dimensional mechanical contact model. The input values for the

roughness of the rigid surface are discrete data points from a computed or measured rough surface. The roughness of the elastic layer is applied as an offset to an initial vertical position of a point mass. The point-masses are connected by spring-, damper- and Maxwell-elements in vertical and horizontal direction. They are also coupled by spring-, damper and Maxwell-elements to the excitation vertically and horizontally. A Maxwell element can simulate the dynamic stiffening of the viscoelastic material as described in the chapter before [8]. The coordinates of the excitation displacement relative to the inertia frame are $u(t)$ and $w(t)$.

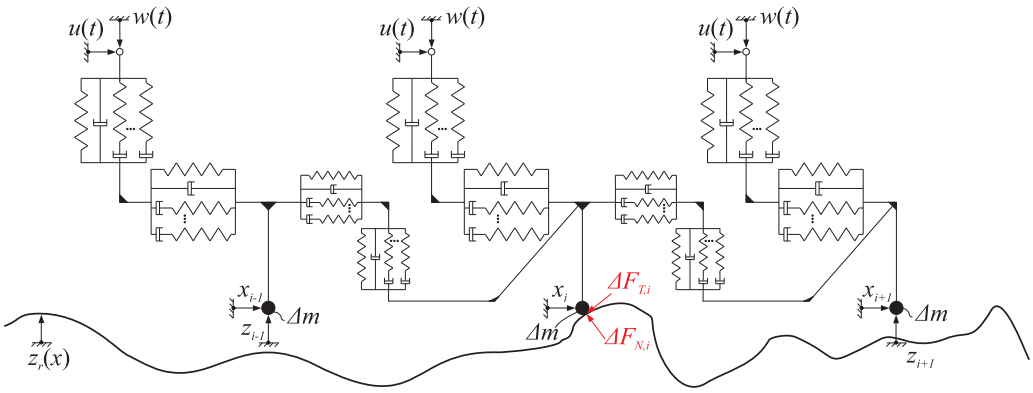

Figure 4: Two-dimensional contact model.

A point-mass without contact has two degrees of freedom, one in the x-direction and one in the z-direction. The equations of motion for an element i are

$$\Delta m_i \ddot{x}_i + F_{c,d,x} + F_{maxwell,x} + F_{c,d,x,l_{i-1\to i}} + F_{maxwell,x,l_{i-1\to i}} - F_{c,d,x,l_{i\to i+1}} - F_{c_{maxwell},x,l_{i\to i+1}} = 0, \tag{3}$$

$$\Delta m_i \ddot{z}_i - F_{c,d,z} - F_{maxwell,z} - F_{c,d,z,l_{i-1\to i}} - F_{maxwell,z,l_{i-1\to i}} + F_{c,d,z,l_{i\to i+1}} + F_{c_{maxwell},z,l_{i\to i+1}} = 0. \tag{4}$$

The equations contain the corresponding spring and damper forces $F_{c,d}$ acting through the external excitation and the adjacent elements on the mass. Furthermore, the force components $F_{maxwell}$ of the n Maxwell-elements are added. The index l describes the coupling between the masses. The number of the Maxwell-elements can be arbitrarily selected, so the model is adaptable to various materials. Every Maxwell element has an internal variable y and is described by a differential equation of 1st order.

Once, an element comes into contact, the equations change. The element can now only move tangentially to the roughness, thus the point-mass has only one degree of freedom.The variable s_i describes the slope at the contact point of the mass Δm_i,

$$s_i = \tan(\varphi_i) = \left.\frac{\partial z_r(x)}{\partial x}\right|_{x=x_i}. \tag{5}$$

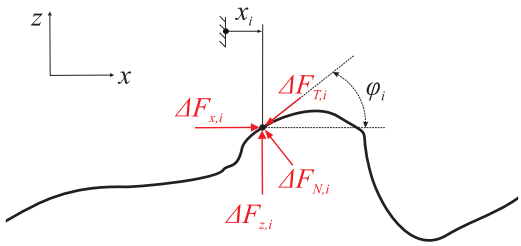

Figure 5: Forces in the contact zone.

The new equation of motion can be derived considering kinematics and the forces acting on the point-mass as depicted in Figure 5. This results in the equations

$$\Delta F_{x_i} = -\frac{\Delta F_{T_i}}{\sqrt{1+s_i^2}} - \frac{\Delta F_{N_i} s_i}{\sqrt{1+s_i^2}}, \tag{6}$$

$$\Delta F_{z_i} = -\frac{\Delta F_{T_i} s_i}{\sqrt{1+s_i^2}} + \frac{\Delta F_{N_i}}{\sqrt{1+s_i^2}}. \tag{7}$$

Rearranging the equation 7 and inserting into equation 6 yields the relation

$$\Delta F_{x_i} + \Delta F_{z_i} s_i = -\Delta F_{T_i} \sqrt{1+s_i^2}. \tag{8}$$

The forces ΔF_{x_i} and ΔF_{z_i} are calculated from the left side of equations 3 and 4. The location of the point-mass in the z-direction and its derivatives are as follows

$$z_i = z_r(x_i), \qquad \dot{z}_i = \frac{\partial z_r}{\partial x}\dot{x}_i, \qquad \ddot{z}_i = \frac{\partial^2 z_r}{\partial x^2}\dot{x}_i^2 + \frac{\partial z_r}{\partial x}\ddot{x}_i. \tag{9}$$

The complete model can described by the system of equations

$$\mathbf{M}\ddot{\mathbf{r}} + \mathbf{D}\dot{\mathbf{r}} + \mathbf{C}\mathbf{r} = \mathbf{B}\mathbf{r}_{\mathbf{exc}} + \mathbf{F}. \tag{10}$$

With the displacement vector

$$\mathbf{r} = [z_1 \ldots z_n \; x_1 \ldots x_n \; \mathbf{y}]^T \tag{11}$$

and the excitation vector

$$\mathbf{r}_{\mathbf{exc}} = [w(t) \; u(t) \; \dot{w}(t) \; \dot{u}(t)]^T. \tag{12}$$

The vector $\mathbf{y}$ within the displacement vector contains the internal variables of each Maxwell elements. Mass matrix $\mathbf{M}$, damping matrix $\mathbf{D}$, stiffness matrix $\mathbf{C}$ and excitation matrix $\mathbf{B}$ are

divided into separate sub-matrices because these can be generated automatically in Matlab due to their simple structure, with

$$\mathbf{M} = \begin{bmatrix} \mathbf{M_{11}(r)} & \mathbf{0} \\ \mathbf{0} & \mathbf{0} \end{bmatrix}, \quad \mathbf{D} = \begin{bmatrix} \mathbf{D_{11}(r)} & \mathbf{0} \\ \mathbf{D_{21}} & \mathbf{D_{22}} \end{bmatrix}, \tag{13}$$

$$\mathbf{C} = \begin{bmatrix} \mathbf{C_{11}(r)} & \mathbf{C_{12}(r)} \\ \mathbf{C_{21}} & \mathbf{C_{22}} \end{bmatrix}, \quad \mathbf{B} = \begin{bmatrix} \mathbf{B_{11}(r)} & \mathbf{B_{12}(r)} \\ \mathbf{B_{21}} & \mathbf{B_{22}} \end{bmatrix}. \tag{14}$$

The matrices $\mathbf{M_{11}}$, $\mathbf{D_{11}}$, $\mathbf{C_{11}}$, $\mathbf{C_{12}}$, $\mathbf{B_{11}}$ and $\mathbf{B_{12}}$ include the parameters of the equations of motion. The Matrix $\mathbf{C_{12}}$ couples the equations of motion with Maxwell elements. The variables of Maxwell elements are determined by the sub-matrices of the second line. Due to the contact condition of equation 7, the matrices in the first line become position-dependent. Furthermore, due to the contact conditions all matrices are variable in their dimension.

For no point mass in contact, the system has the maximum order $2k + 4kn - 2n$. After applying the contact constraints, the system order and also the system matrices are reduced. The number of internal variables of Maxwell elements remains unchanged, while the degrees of freedom of the masses are variable. The new dimension of the displacement vector is $(2k - k_{contact}) + 4kn - 2n \times 1$.

For simulation the movement differential equations and the differential equations of Maxwell-elements are transformed into a state space. The system equations have the following structure

$$\begin{bmatrix} \dot{\mathbf{r}} \\ \ddot{\mathbf{r}} \\ \dot{\mathbf{y}} \end{bmatrix} = \begin{bmatrix} \mathbf{0} & \mathbf{I} & \mathbf{0} \\ -\mathbf{M_{11}(r)^{-1}C_{11}(r)} & -\mathbf{M_{11}(r)^{-1}D_{11}(r)} & -\mathbf{M_{11}(r)^{-1}C_{12}(r)} \\ -\mathbf{D_{22}^{-1}C_{21}} & -\mathbf{D_{22}^{-1}D_{21}} & -\mathbf{D_{22}^{-1}C_{22}} \end{bmatrix} \begin{bmatrix} \mathbf{r} \\ \dot{\mathbf{r}} \\ \mathbf{y} \end{bmatrix} + \begin{bmatrix} \mathbf{0} \\ -\mathbf{M_{11}(r)^{-1}F} \\ \mathbf{0} \end{bmatrix} + \mathbf{U_{exc}}. \tag{15}$$

The simulation of the contact model is performed using an ODE solver. First of all the corresponding matrices of the state space model are automatically generated in consideration of the initial states. Than the calculation starts with the given initial values and continues until a termination condition is reached. This is the case when a point-contact with the roughness profile comes into contact, or when the normal force of an element becomes equal to zero. The system matrices are adapted to the new contact conditions and initial values. Subsequently, the simulation restarts. Figure 6 shows the simulation process.

5 MODEL RESULTS

In the following, some results of the model are presented. For this purpose, a special case is assumed whereby the model is simplified. The Maxwell-elements are disabled, so only spring and damper act between the masses and the external excitation. In the simulation, a rough rigid surface is vertically pressed against a smooth elastic surface. This process is terminated as soon as a selected nominal pressure is reached. Then a tangential movement of the elastic body on the roughness at low speeds is performed.

Figure 7 shows that the tangential contact stiffness increases when the surface pressure rises. The reason for the increase in stiffness is the higher number of contacting elements. Sliding of all elements is reached when the tangential force no longer increase.

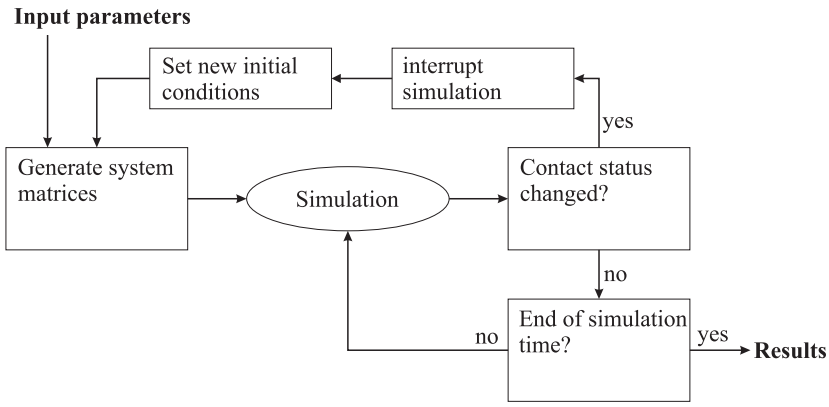

Figure 6: Simulation chart.

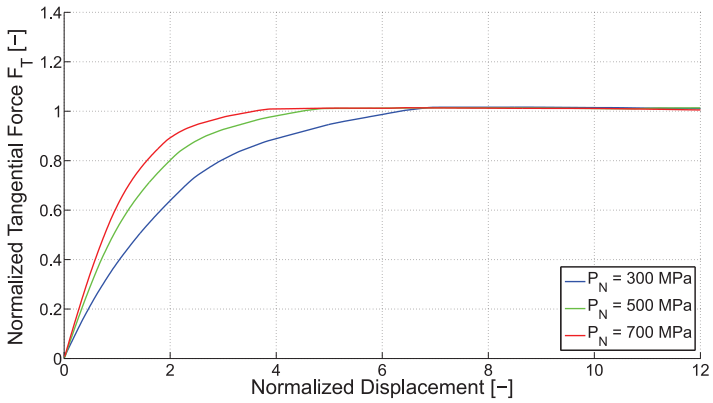

Figure 7: Tangential Force-Displacement Relation.

6 CONCLUSION

Within this work a contact model has been presented to simulate the hysteretic component of rubber friction. The model can discribe the contact behavior on a small length scale. It is possibel to use the results of these simulations for ponit-contact elements, in order to simulate the entire contact surface with unequally distributed normal pressure on a larger scale. For this, the simulation results are stored in lookup tables. The model can correctly represent the viscoelastic material properties, described by the storage and loss modulus. Through the knowledge whether an element is in contact or not, it is possible to draw conclusions about the true contact area. This can be incorporated into an approach for modeling the adhesive friction.

REFERENCES

[1] W.E. Meyer and H.W. Kummer, Die Kraftbertragung zwischen Reifen und Fahrbahn. *ATZ Automobiltechnische Zeitschrift 66, 245–250, 1964.*

[2] P. Moldenhauer, *Modellierung und Simulation der Dynamik und des Kontakts von Reifenprofilbloecken*. Dissertation, Freiberg, 2010.

[3] W. Sextro, *Dynamical Contact Problems with Friction*. Springer Verlag, Berlin, 2007.

[4] B. Lorenz, B.N. Persson, G. Fortunato, M. Giustiniano and F. Baldoni, Rubber friction for tire tread compound on road surfaces. *Journal of Physics: Condensed Matter 25, 2013.*

[5] J. Neuhaus and W. Sextro, A Discrete 2D Model for Dynamical Contact of Rough Surfaces. *3rd International Conference on Computational Contact Mechanics 2013, Lecce, Italy, 51–53, 2013.*

[6] J. Neuhaus and W. Sextro, A Discrete Model for Dynamical Simulation of Normal and Tangential Contact on Rough Surfaces. *Congresss on Numerical Methods in Engineering 2013, Bilbao, Spain, 2013.*

[7] J. Neuhaus and W. Sextro, A Two Dimensional Model for the Dynamical Contact of Elastic Rough Surfaces. *Proceedings in Applied Mathematics and Mechanics Vol.14, 227–228, 2014.*

[8] M. Lindner, W. Sextro, K. Popp, Hysteretic Friction of a Sliding Rubber Element. *Proceedings in Applied Mathematics and Mechanics Vol.4, 101–102, 2004.*